*Paper 28*

# Towards Geologically Realistic Inversion

Fullagar, P. K. [1], Pears, G. A. [2]

1. Fullagar Geophysics Pty Ltd, Brisbane, Queensland, Australia
2. Mira Geoscience Asia Pacific Pty Ltd, Brisbane, Queensland, Australia

**ABSTRACT**

*During the past 10 years there has been a shift in geophysical interpretation away from idealised geometrical bodies floating in air and towards fully three-dimensional models. This transition has been driven by a number of factors, both technological and conceptual. The principal conceptual driver has been the growing recognition of the importance of integrated interpretation. Interpretation is a shared responsibility of geoscientists, the common goal being an Earth model consistent with all available information. Inversion is a numerical process whereby an initial model is adjusted in order to improve the degree of agreement, or fit, between the measured geophysical data and the corresponding calculated data. Petrophysical properties provide the link between geophysics and geology, but this link is indirect. Most 3D inversion programs operate on quantitative "property only" models, which define a distribution of one or more physical properties in the sub-surface. After inversion of pure property models, geology must be inferred from the rock properties. Geological models are categorical, insofar as the sub-surface is divided into rock type domains. In order to capture both geology and petrophysics, a model must be both categorical and quantitative. Such 'geo-physical' models are a force for integration in their own right, and also offer a number of practical advantages over pure property models. In particular, the topological significance of geological boundaries is maintained, permitting geometry inversion as well as property inversion. Analysis of geophysical data alone is not sufficient to fully prescribe the sub-surface distribution of rock properties. Geological and petrophysical information, primarily derived from drill holes, is required in order to reduce uncertainty. "Ground truth", in the form of drill hole pierce points, is imposed explicitly during geometry inversion as fixed points on the geological surfaces. Likewise, petrophysical measurements, if any, locally constrain the rock properties. In addition to these "hard" constraints, petrophysical data can if available in sufficient quantity, constitute a basis for statistically characterising and constraining the property distribution. Otherwise, "soft" constraints can be imposed in the form of a priori weights, e.g. to condition the depth and shape of causative bodies. Geologically-constrained inversion of gravity and magnetic data is illustrated below using a 3D potential fields inversion program interfaced to a 3D geological modelling package. Three examples are described, covering greenfields depth-to-basement (geometry) inversion over a large area, combined geometry and property inversion over a lightly drilled exploration prospect, and property inversion for brownfields exploration over the Cannington mine. Petrophysical property modelling in the mining industry is still fairly rudimentary overall. This is more a reflection on the state of the data than on the state of the art: modelling software exists, but petrophysical data is often inadequate or completely absent. In the next ten years, greater volumes of petrophysical data will support an expanded role for geostatistics. The stronger emphasis on petrophysics will be driven not only by the need for more sophisticated rock property modelling, but also by the demands of managers to quantify the uncertainty in interpretation.*

## INTRODUCTION

During the past 10 years there has been a shift in geophysical interpretation away from idealised geometrical bodies floating in air and towards fully three-dimensional models. This transition has been driven by a number of factors, both technological and conceptual. The key technological drivers have been the on-going advances in computer hardware, geological modelling and visualisation software, geophysical modelling and inversion software, and data quality. The principal conceptual driver has been the growing recognition of the importance of integrated interpretation. Geologists need to incorporate geophysical results into their models in order to explore at all depths in greenfields areas, between drill holes in brownfields areas, and at greater depths in all areas. Geophysicists must constrain their models with geological observations in order to reduce the ambiguity inherent in their interpretations. The common goal is a model consistent with all available information, one which is jointly owned by all geoscientists (McGaughey, 2006).

Petrophysical properties provide the link between mineralogy and geophysics, and hence between geology and geophysics. Rock properties can be measured on drill core or hand samples, or logged downhole. In many mineralised environments, the rock types of interest can be distinguished on the basis of their physical properties. However, lack of knowledge of physical

In "Proceedings of Exploration 07: Fifth Decennial International Conference on Mineral Exploration" edited by B. Milkereit, 2007, p. 444-460

properties is, unfortunately, still the norm in the mining industry. Some progress has been achieved in recent years, both in terms of raising awareness of rock properties and in compiling legacy data, but the mining industry as a whole remains to be convinced of the benefits which could flow from routine collection of petrophysical data. In terms of density, this scepticism is astounding, given that a knowledge of density is fundamental for reserve and resource modelling. Knowledge of density and other rock properties can deliver many benefits at mines (Fullagar, 2000), as well as reduce uncertainty in survey design and interpretation.

Inversion is a numerical process whereby an initial model is adjusted in order to improve the degree of agreement, or fit, between the measured geophysical data and the corresponding calculated data. At minimum, a geophysical model must define a distribution of one or more physical properties in the sub-surface. An inversion procedure which modifies only the properties of model cells is termed property inversion. The well known University of British Columbia programs, MAG3D (Li & Oldenburg, 1996) and GRAV3D (Li & Oldenburg, 1998), perform property inversion.

Geological models are comprised of surfaces, mainly litho-stratigraphic boundaries and structures, which divide the ground into rock type domains. The surfaces are interpolated between mapped or drilled points on geological contacts and structures. In order to integrate geological and geophysical interpretation as closely as possible, it is advantageous to incorporate geological observations and surfaces in geophysical models, and to manipulate the surfaces during inversion. An inversion process which modifies the shape of geological boundaries is termed geometry inversion. Geometry inversion which honours geological observations can be regarded as a form of geological modelling; the inversion output is a set of revised surfaces. Programs capable of geometry inversion can also perform property inversion, either simultaneously, e.g. MCMC (Bosch et al., 2006), or sequentially, e.g. VPmg (Fullagar et al., 2000, 2004, 2006).

Geological models are categorical, insofar as each sub-surface domain is assigned to a rock type. For geometry inversion, the geological significance of each model cell boundary must be defined, i.e. each cell must be attributed with a rock type as well property value(s). Therefore a categorical model is a pre-requisite for geometry inversion. In addition to their suitability for geometry inversion, categorical models offer several other advantages. Firstly, a categorical model is both a geology model and a property model, whereas geology must be inferred from the rock properties after inversion of a pure property model. This can be both time consuming and subjective, e.g. when sharp, well-drilled contacts become smeared as a result of pure property inversion. Secondly, algorithms operating on categorical models can exert a greater degree of control over rock properties. In particular, different magnetic remanence parameters or statistical distributions can be assigned according to rock types. Thirdly, categorical models permit flexibility in the conduct of inversion, e.g. allowing changes to be confined to selected rock types or contacts. Adoption of a categorical model structure does not limit options for property inversion: "unconstrained" property inversion can be performed on a categorical model, with changes restricted to specific units or permitted throughout the entire sub-surface.

Geophysical data alone are not sufficient to fully prescribe the sub-surface distribution of a rock property. Geological information is required in order to reduce uncertainty. Drill core usually constitutes the principal source of primary geological data. Drill holes are also the primary source of rock property data. In categorical models any drill hole pierce points, i.e. known 3D locations where drillholes intersect geological contacts or structures, can be incorporated explicitly (within model resolution), and held fixed during geometry inversion. In this way, the "ground truth" is captured and, at the same time, the more subjective, interpreted regions of the geological surfaces are always identified.

If downhole or drill core property measurements are available, certain points in the model can be regarded as known, in direct analogy to pierce points. The known small scale property values can be expressed in the model as fixed property cells provided the difference in volume (or "support") between core samples and model cells is taken into account. Upscaling is a familiar consideration in mining geostatistics, but the assumption of additivity is untenable for some petrophysical properties, e.g. conductivity (Close et al., 2001). If property measurements are available in sufficient numbers over a representative volume, statistical and geostatistical conditioning of the sub-surface property distribution becomes viable. Integration of geophysical inversion and geostatistical modelling is well advanced in the context of petroleum exploration and production, e.g. Dubrule (2003), and algorithms suitable for mining applications are under development. Thus rock property data can constrain the property distribution both locally, by "freezing" individual model cells, and globally within entire domains by statistically and geostatistically characterising the property within each rock type.

The distribution of physical properties is always conditioned during property inversion, even in greenfields applications when there are no drill holes. The most common forms of a priori conditioning are upper and lower bounds, and weighting to favour certain characteristics, e.g. preferred source depths, shapes, and orientations, or overall degree of smoothness (Li & Oldenburg, 1996, 1998; Chasseriau & Chouteau, 2003).

Geologically-constrained inversion of gravity and magnetic data is illustrated herein using a 3D potential fields inversion program, VPmg (Fullagar Geophysics Pty Ltd), interfaced to a 3D geological modelling package, Gocad (Earth Decision Sciences Inc). VPmg model parameterisation, inversion methodology, and geometry and property constraints are introduced in the next three sections. Three examples are described, from exploration projects and a mine site in the Mt. Isa region, Queensland. The first example is a regional depth to basement interpretation, to illustrate geometry inversion in a greenfields exploration context. Combined geometry and property inversion is illustrated in the second example, in the context of magnetic inversion over an exploration prospect. Sparse drilling imposes constraints on both the shape and the susceptibility of the magnetic sources. The third example illustrates brownfields exploration at mine scale: ground magnetic data over Cannington is inverted. The geological structure is assumed known and property inversion is employed to reconcile the magnetic anomaly. The key conclusions are that inversion based on categorical models is blurring the distinction between geological and geophysical interpretation, and that improved petrophysical characterisation is required in order for integrated interpretations to bear a closer resemblance to geological reality.

## A METHODOLOGY FOR 3D GEOLOGICALLY-CONSTRAINED INVERSION

The basic structure of a categorical model is illustrated in Figure 1. Categorical models are essential for geometry inversion, since a geological boundary separates one rock domain from another by definition. Therefore, the bounding surfaces do not exist in the model until each cell is assigned to a rock type.

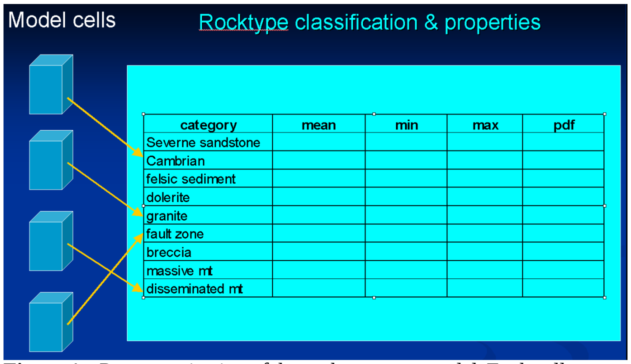


**Figure 1:** Parameterisation of the rock property model. Each cell belongs to a rock type. Its physical properties are then assigned accordingly.

Once each volume element ("cell") in the model has been classified, its physical properties are attributes not only of the individual cell, but also of the class as a whole. If a geological unit is homogeneous, all its constituent cells share the same property value. On the other hand, if a geological unit is heterogeneous, the property values of all its cells should collectively conform to the appropriate probability density function (pdf). Unfortunately, all too frequently in mining applications, the statistical variability of physical properties is not well characterised.

Modification of geological boundaries can be achieved either by re-classifying cells with cell boundaries fixed ("cell defection"), or by moving the cell boundaries with cell rock types invariant. In the former case, the underlying model mesh is unchanging, and boundaries shift in discrete jumps of one or more cells. In the latter case, the mesh deforms, and arbitrarily small boundary adjustments are permitted. The cell defection style of boundary adjustment lends itself to stochastic inversion: random cell re-classifications are introduced, tested against geological and geophysical criteria, and then accepted or rejected. Some algorithms allow both styles of boundary modification (Bosch et al, 1999).

In this paper, we will explore a deforming mesh style of geometry inversion. Viewed in plan, the sub-surface will be discretised into close-packed identical rectangular prisms. Prism tops honour surface topography, and internal horizontal contacts divide each prism into cells. Viewed in section, the vertical dimensions of the cells are arbitrary (Figure 2): the mesh adapts to the local geology. Thus a 0.2m thick cell can abut a 200m thick cell. During geometry inversion, continuous movement of the horizontal cell boundaries is permitted, but vertical prism walls are fixed. This type of "adaptive mesh" has been implemented in VPmg. The geological units can be heterogeneous or homogeneous.

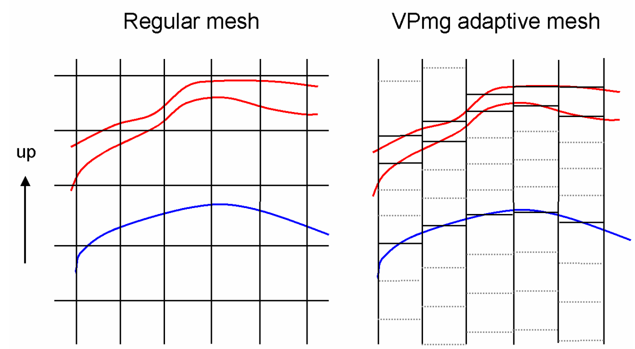


**Figure 2:** Schematic model sections illustrating the differences between a conventional fixed mesh (left) and the deforming mesh implemented in VPmg. Sub-cells (dotted boundaries) can differ in size from one rock type to another.

The VPmg adaptive mesh represents a compromise between generality and practicality. It offers several advantages over a conventional regular mesh:

i. details in geological models, especially thin geological units, can be retained in the rock property model;
ii. all surfaces, including the ground topography, can be represented more accurately; and
iii. the adaptive mesh is more compact, i.e. far fewer cells are required (especially for homogeneous units), so inversion run times are shorter.

Within each unit the property can be homogeneous or vary from cell to cell. If greater intra-unit resolution is desired, the cells can be vertically divided into sub-cells with specified dimension (Figure 2). The vertical dimension specified for the sub-cells can differ from unit to unit.

In some circumstances it is advantageous to apply geometry inversion to bodies defined within a variable background which is defined on a regular mesh. In such cases, an adaptive mesh can co-exist with a static mesh. Cells in the regular mesh shrink and perhaps disappear if the target body expands, or conversely reappear and perhaps resume their full size if the body contracts. Base-of-salt geometry inversion within a pre-defined density distribution is one important application of co-existing meshes in petroleum exploration (Fullagar et al., 2006).

### Inversion Algorithm

#### Steepest Descent Inversion

The inverse problem is usually solved using the method of steepest descent in VPmg. The inversion per se is therefore fast, because no matrix inversion is required. Inversion terminates when an "acceptable" fit has been achieved. In VPmg, a chi-squared condition has been adopted: the fit is deemed to be acceptable when $x^2$ where

$$\chi^2 = \frac{1}{N}\sum_{n=1}^{N}\left(\frac{o_n - c_n}{\varepsilon_n}\right)^2$$

and where N is the number of data, $\{o_n\}$ are the observed data, $\{c_n\}$ are the calculated data, and $\{\varepsilon_n\}$ are the corresponding data uncertainties. Inversion will also terminate if successive iterations do not produce any appreciable reduction in misfit; this is a "stall", usually indicating that constraints must be relaxed in order to achieve a satisfactory fit to the data.

#### Stochastic inversion

Property inversion of heterogeneous units can be performed in VPmg, optionally, via a simple statistical approach. In stochastic inversion, random perturbations are chosen for each cell of each active unit in turn, e.g. Lane et al. (2006). The size of the random perturbations is governed by the property distribution for the unit to which the cell belongs. The perturbation is accepted if it reduces the chi-squared misfit, and is rejected otherwise. The specified 'bounds' define the three standard deviation limits from the mean.

## GEOMETRY CONSTRAINTS

In the context of geometry inversion, "unconstrained inversion" usually denotes an absence of fixed points, usually drill hole pierce points, on the geological boundaries. However, geometry inversion is always constrained to some extent. In VPmg the horizontal cell boundaries are prevented from erupting through the ground surface, or from passing through one another. In addition, the algorithm is conditioned to suppress large changes at shallow depths. Rock properties also constrain geometry inversion: a boundary associated with zero property contrast will not move.

Beyond these general constraints, it is possible to impose constraints on specific geological surfaces. When drill holes exist, it is essential to capture and preserve "ground truth" in the rock property model; as explained below, this is achieved in VPmg by means of both "hard" constraints (pierce points and bounds) and "soft" constraints (weights). In the absence of drill holes, it is still desirable to enable the user to hold some surfaces (or portions of surfaces) fixed while allowing others to vary. Accordingly, user-defined constraint flags can be set in VPmg model files.

### Pierce point constraints

Preservation of drilled contact positions during inversion is a fundamental pre-requisite for integrated interpretation. The aim of 3D inversion is to build on the existing knowledge of the geology; so honouring pierce points can be viewed as a requirement for geological credibility. At the same time, drillhole pierce points are enormously advantageous insofar as they reduce the inherent ambiguity of potential field interpretation.

In VPmg, horizontal cell boundaries are held fixed if pierced by a drill hole. If only a few vertical drill holes are involved, finding and tagging the fixed cell boundaries is straightforward in an editor. As the number of drill holes increases, especially if the holes are inclined away from vertical, and as the geology becomes more complex, tagging the fixed contacts is impracticable without suitable software. To address this need, Mira Geoscience has developed utilities in Gocad to impose drilling-based constraints in VPmg model files.

If a pierce point lies close to the centre of a horizontal contact, there is no confusion as to which VPmg cell boundary should be fixed, especially if dips are gentle (Figure 3a). However, if the actual pierce point is located at or near the edge of a VPmg prism, assigning interfaces as fixed or free becomes more subjective. The simple binary fixed/free designation becomes inadequate as dips increase, since a pierce point may be a long way above or below the nearest VPmg interfaces that represent the geological contact in question (Figure 3b).

One response to these detailed considerations is to introduce "activation distances" around each pierce point, and to fix the interfaces which lie within range. Thus in Figure 3b, contact A is deemed to be within range of pierce point P. More generally, the need to limit the vertical movement of prism boundaries above and below the trace of a drill hole has been identified. These limits on travel are termed "bound constraints".

Cells with known property, e.g. cells intersected by a drill hole which has been logged for density, are normally fixed in size. This is because the property value assigned to a rock volume is a function of both the position and size of that volume. Consequently, the upper and lower interfaces of known-property cells are fixed in VPmg.

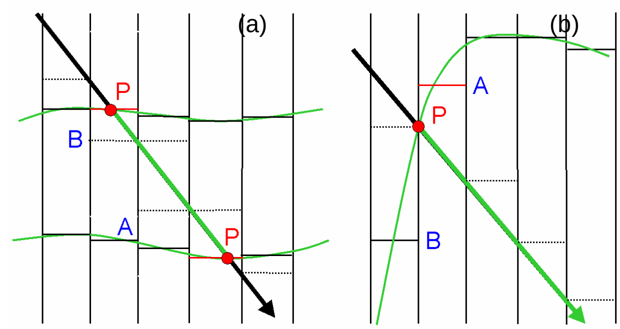


**Figure 3:** Schematic sections to illustrate the origin of bound constraints. Thick oblique line represents a drill hole. Fixed cell boundaries are coloured red; bound constraints are dotted. Pierce points, P, on the upper and lower contact of a particular unit (green) are marked with a red dot. In panel (a), the dotted line at B marks the upper limit of travel for the interpreted contact at A. In panel (b), the contact at A is deemed to be sufficiently close to P to remain fixed, while the dotted line at P marks the upper limit of travel for the interpreted contact at B.

### Bound Constraints

As foreshadowed above, designating contacts as either fixed or free is inadequate for imposing drill constraints on VPmg models. Rather, pierce points and drill trajectories must sometimes be expressed as bounds on the travel of free interfaces. Bound constraints are most likely to arise when dips are steep or when drill holes are inclined from the vertical. In Figure 3a, a continuous intersection of a particular geological unit (coloured green) has been logged between the two pierce points (P). Therefore, the interpreted contact at A cannot move higher than B. Similarly, in Figure 3b the pierce point at P defines an upper limit for the model interface currently at B.

Upper bound constraints also arise when contacts are interpreted to lie below the reach of drilling. Similarly, a contact interpreted to occur within a percussion pre-collar can be bounded below, e.g. where core drilling commences.

Bound constraints are represented in VPmg models as artificial interfaces, distinguishable from the geological interfaces.

### Soft Geometry Constraints

The manner in which a geological surface is interpolated between known mapped or drilled points is subjective. Just as an individual interpreter exercises judgement or imposes bias, so too a computer program must invoke subjective ("soft") criteria to define the preferred shape of a geological contact between known points. It is possible to distinguish two aspects of this interpolation process: defining the neighbourhood of influence of individual fixed points; and imposing a certain character on the contact surface. In principle, quite sophisticated criteria could be invoked to constrain the geometry of the contact, e.g. favouring variations of a particular wavelength or strike. However, attention is restricted to a simple distance weighting here.

In VPmg the radius of influence of a pierce point is defined as its depth or the distance to the nearest pierce point, whichever is smaller. The movement of each unconstrained ("free") interface within this radius is damped during inversion. The damping is achieved by applying weights to the derivatives associated with each free interface; the derivatives encapsulate the sensitivity of each data point with respect to changes in elevation of a free interface. The weights are multiplicative. For the *j*th free interface lying distance $r_{jk}$ from the *k*th pierce point, the weight $w_j$ is updated by the factor $r_{jk}/R_k$, where $R_k$ is the radius of influence of the *k*th pierce point (Figure 4). Thus

$$w_j = \prod_k \frac{r_{jk}}{R_k}$$

provided. $r_{jk} < R_k$. Free interfaces which are far removed from any fixed points are not implicated, i.e. their derivatives are assigned unit weight.

The net effect of the weighting is to de-sensitise the inverse problem to movement of free interfaces within the neighbourhood of fixed interfaces; free interfaces far from fixed interfaces will be moved in preference. This approach is simple and effective, but is by no means the only way for the influence of drill hole pierce points to propagate through the model volume.

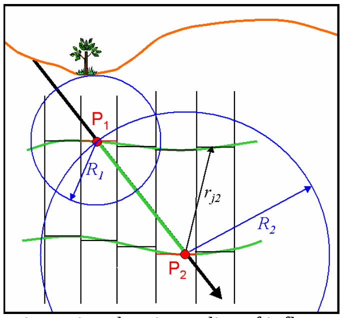


**Figure 4:** Schematic section showing radius of influence around pierce points, within which geometry changes are damped during inversion. In VPmg, R is defined as the lesser of depth and distance to nearest pierce point.

## ROCK PROPERTY CONSTRAINTS

In the context of property inversion, the term "unconstrained inversion" usually signifies that the starting model is homogeneous. The terminology is misleading, since property inversion is always constrained to some extent. Individual algorithms impose constraints implicitly, e.g. depth weighting (Li & Oldenburg, 1996, 1998) to avoid "equivalent stratum" models with all fluctuations in density or susceptibility concentrated at shallow depths. In addition, many algorithms are conditioned to favour smoothly varying property distributions.

Explicit property constraints can be applied to all model cells or to subsets of cells, e.g. the cells comprising a particular geological unit. For example, the property within a particular geological unit can be constrained to lie within prescribed upper and lower bounds. When rock properties have been logged downhole or measured on drill core, it is desirable to incorporate this information in the rock property model. In VPmg this is achieved by means of both hard constraints (fixed property cells) and soft constraints (weights). In the absence of drill holes, it is still desirable to enable the user to control which cells are fixed and which are allowed to vary. User-defined weights serve this purpose in VPmg and other programs, e.g. GRAV3D and MAG3D.

### Homogeneous Property Constraints

In VPmg it is possible to hold the density or susceptibility uniform within a given geological unit, and hence to examine the degree to which the data can be explained by inter-unit variability alone. Each homogeneous unit can be designated as active or inactive during inversion; in active units, upper and lower bounds define the permissible range of property values. Homogeneous units are adequate in many contexts, e.g. for recent cover (including water or ice) over dense basement. Even for geological units which are not uniform in properties, the assumption of homogeneity is often a useful starting point when very little is known about local rock properties; inversion can then define the optimal "mean" property. Intra-unit variability can be allowed to develop subsequently, if necessary.

Homogeneous property inversion is fast, even if the model large and geometrically complex, because there are only a handful of active parameters. The inversion problem per se is therefore small.

### Property Bound Constraints

Upper and lower bounds are the simplest and most common constraints imposed on cell properties. Property bounds can be applied globally, to all cells, or different bounds can be applied to sub-sets of cells, e.g. those belonging to individual geological units. Some programs, e.g. GRAV3D and MAG3D, can impose different bounds on every cell.

### Drilled cell constraints

If rock properties are allowed to vary from cell to cell, i.e. if geological units are heterogeneous, then property measurements from downhole logs or from core measurements can be honoured during inversion. Normally, the property of a model cell is fixed if petrophysical measurements are located within it. As for pierce points, finding and tagging the fixed property cells is usually impractical without purpose-written utilities.

However, constrained property inversion is an inherently complex undertaking. The key issues are uncertainty and scale. Uncertainty encompasses both consistency (precision) and accuracy (bias). Consistency is often difficult to achieve; for example, core susceptibility data is not infrequently collected by different people at different times with different equipment in holes or on core of different diameter. Accuracy depends on instrumental sensitivity and calibration, as well as on quality of survey documentation (“meta data”), e.g. unit of measurement.

Measurements on core relate to very small volumes of rock, say 5 x 10-3 m3; downhole logs relate to considerably larger, albeit still small, volumes, say 0.5 m3; but the cells comprising a typical block model for inversion are immense by comparison, e.g. 1000 m3 contained within a cube with side 10 m. The property assigned to the model cell must be derived from the smaller scale measurements. For density, conventional linear “up-scaling” algorithms are appropriate, e.g. Oz et al. (2002). Linearity or additivity is usually an acceptable approximation for magnetic susceptibility also, except when self-demagnetisation is important or remanence is strong and variable.

In view of these considerations, the value attributed to a known-property model cell is always somewhat uncertain in practice. The user can decide whether to hold its value absolutely fixed during inversion or to allow it to vary, e.g. by applying a weight proportional to the standard deviation.

### Soft property constraints

It is desirable to limit property changes in the vicinity of fixed cells, since rock properties usually exhibit a degree of correlation over a certain length range. In VPmg, weights are applied to derivatives so that a change in property is penalised if a cell has a low weight. The weights can either be imposed a priori or by default. The VPmg default weights are based on the notion of radius of influence, as described in Section 3.3 above. The effect of the radius of influence is sometimes evident around isolated holes (Figures 13 & 15). The a priori weights are computed externally, e.g. standard deviations of rock property for each model cell, derived via kriging, could be adopted as weights.

## EXAMPLES OF 3D GEOLOGICALLY-CONSTRAINED INVERSION

Examples of constrained inversion are presented in this section, for three data sets recorded in the vicinity of Mt. Isa, Queensland. The applications range from greenfields exploration over the Boulia 1:250,000 map sheet, to exploration over the Bull Creek prospect, to near-mine exploration at Cannington (Figure 5). Given that the inversion objectives and available information differ in each case, the inversion approach is tailored accordingly.

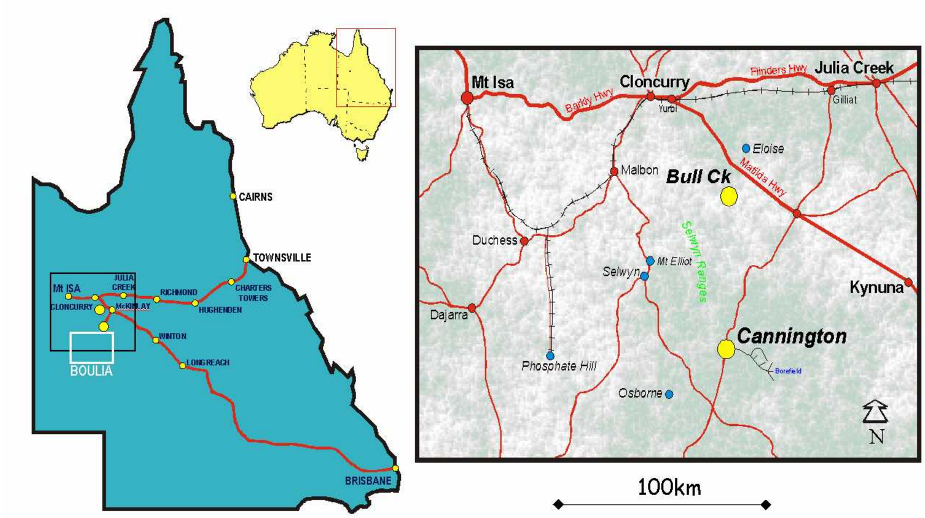


**Figure 5:** Location map, showing Boulia 1:250,000 map sheet (left) and Bull Creek and Cannington in inset (right) near Mt. Isa, Queensland, Australia (courtesy BHP Billiton Minerals).

### Depth to basement inversion, Boulia, Queensland

Paleozoic sedimentary cover thickness strongly influences area selection for exploration in Proterozoic and Archean terranes. Constructing a basement unconformity surface that is consistent with potential field data is a natural greenfields exploration application for geometry inversion.

Depth-to-basement prediction is illustrated here via inversion of gravity data over the Boulia 1:250,000 scale map sheet in western Queensland (Figure 5). The Boulia map sheet occupies an area where the Proterozoic Mt. Isa Inlier plunges gently southwards beneath Palaeozoic sediments of the Georgina Basin. The free-air gravity is depicted in Figure 6. Topographic relief over the entire map sheet is very modest (less than 150m). The Osborne Cu-Au mine is located near the northeast corner of the map sheet.

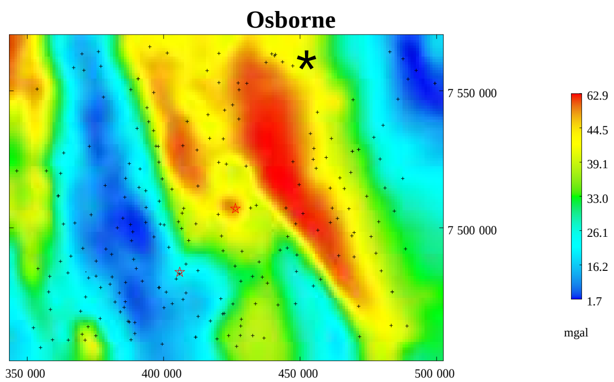


**Figure 6:** Free-air gravity image, Boulia 1:250,000 sheet, Queensland. Drill holes intersecting basement are marked as red stars. Basement depths were 1300m (central) and 530m (SW). Water bore locations are marked with black crosses. (Data courtesy Queensland Department of Natural Resources and Mines).

Interpretation of gravity is fraught with ambiguity. The importance of a priori information during inversion is demonstrated here by inverting the gravity data twice, first without and then with constraints. For the initial "unconstrained" inversion it is assumed that both the Proterozoic basement and the sedimentary cover are homogeneous, with densities 2.80 g/cc and 2.42 g/cc respectively. The basement contact is at a constant elevation initially, at a depth of approximately 700m.

The basement topography after inversion is depicted in Figure 7. Troughs have developed beneath gravity lows and ridges beneath gravity highs. The RMS misfit was reduced from 12.86 mgal to 1.75 mgal. In the absence of additional information, this is a perfectly sensible hypothesis

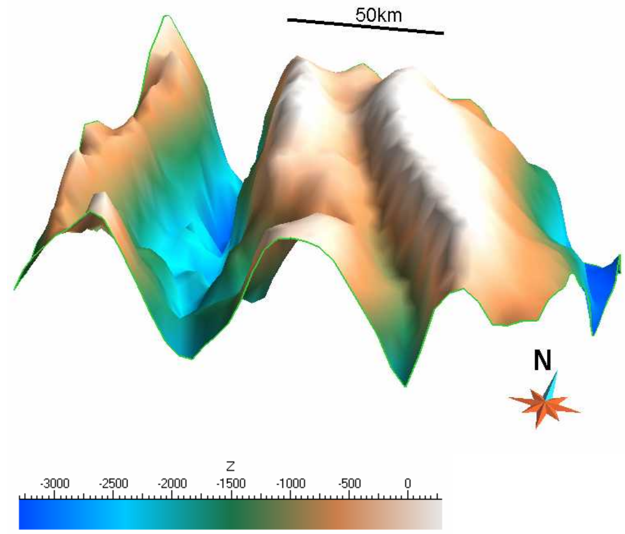


**Figure 7:** Perspective view of the basement surface after unconstrained geometry inversion. The colour depicts elevation (mASL). Vertical exaggeration 1:20.

The uncertainty associated with gravity interpretation can be minimised if all available information is exploited. For Boulia, depth to basement and Proterozoic geology interpretations based on aeromagnetics were available (Figure 8 after Mackey et al., 1999, 2000), as well as a compilation of density values (Hone et al., 1987). In addition, two drill holes were known to have intersected basement (Figure 6).

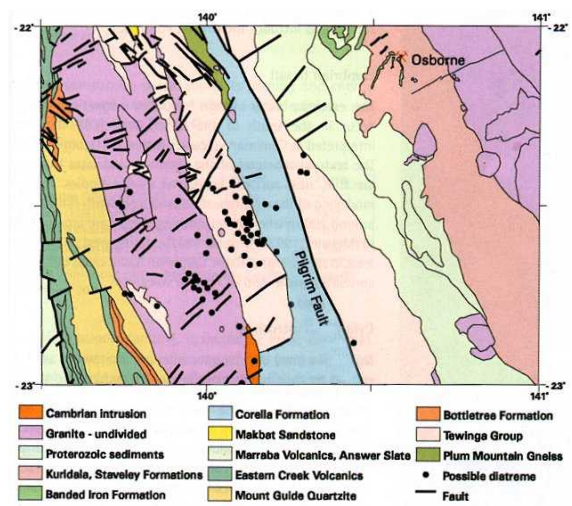


**Figure 8:** Boulia interpreted basement geology (after Mackey et al, 2000).

A 3D starting model was constructed for constrained inversion, with basement elevation conforming with the drill hole pierce points and the aeromagnetic depth-to-source estimates. Density was assigned to interpreted basement domains (Figure 8) in accordance with the density compilation (Table 1). Paleozoic cover was represented as a layer of uniform density (2.42 g/cc) as before. In this model, shallow magnetic basement correlated with low gravity, while denser basement lithologies tended to be more deeply buried.

**Table 1: BOULIA STARTING MODEL DENSITIES**

| Geological Unit | Density (g/cm3) |
|---|---|
| Eastern Creek Volcanics | 2.82 |
| Mount Guide Quartz | 2.72 |
| Cambrian Intrusion | 2.67 |
| Undivided Granite | 2.63 |
| Kuridala, Stavely Formations | 2.70 |
| Corella Formation | 2.75 |
| Makbat Sandstone | 2.65 |
| Marraba Volcanics, Answer slate | 2.72 |
| Bottletree Formation | 2.67 |
| Tewinga Group | 2.68 |
| Plum Mountain Gneiss | 2.66 |
| Banded Iron Formation | 3.10 |

The calculated gravity response of the starting model resembled the observed gravity in qualitative terms, but the data fit was not satisfactory. Basement density inversion was applied first, to address some inconsistencies between interpreted basement lithology and the gravity data. Subsequently, basement topography was adjusted via geometry inversion, with the basement elevation held fixed at the two drill hole pierce points. The basement surface was also bounded above by water bores which terminated in Paleozoic sediments (Figures 6, 9). The basement contact after constrained inversion is depicted in Figure 9. The RMS misfit for this model is 2.9mgal. The data fit can be improved by means of further basement density inversion (Pears et al., 2001).

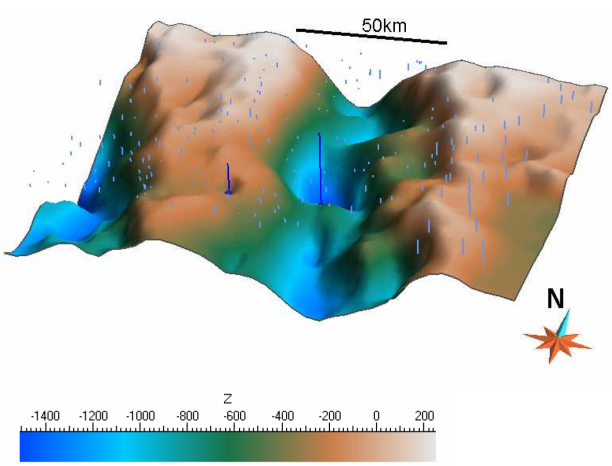


**Figure 9:** Perspective view of the basement contact after constrained geometry inversion, with water bores (blue) and deep drill holes (purple) superimposed. Colour indicates elevation (mASL).

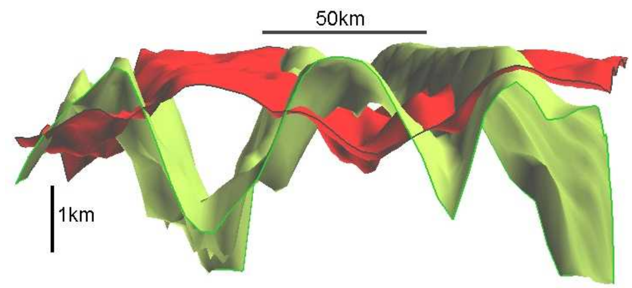


**Figure 10:** Perspective view of inferred basement surface, comparing the results after constrained (red) and unconstrained (green) geometry inversion.

The basement surfaces produced by constrained and unconstrained inversion are compared in Figure 10. The differences are stark: When additional information is utilised, it is revealed that gravity lows are associated with the occurrence of granites and other felsic rocks in the basement rather than an increase in the thickness of sedimentary cover. The constrained surface-based inversion has produced a 3D depth-to-basement model, consistent with all information, which can guide area selection for exploration.

**Combined geometry and property inversion, Bull Creek, Queensland**

The inversion modus operandi adopted for Boulia, involving a sequence of property and geometry inversions, is typical for VPmg. The order in which inversions are applied can affect the final result. Sometimes the most appropriate sequence is obvious, e.g. homogeneous unit inversion before geometry inversion if a contact is well drilled but the property contrast is unknown. In other cases, the order of inversions and even the type of inversions is a matter for subjective judgement. This subjectivity is simply a reflection of the underlying non-uniqueness. Indeed, applying inversions in a different sequence is one way to explore for alternative interpretations.

The gravity response at Boulia can be explained in terms of basement density variations in or in terms of the geometry of the basement unconformity. It is sometimes desirable to allow both geometry and property to change simultaneously. In VPmg, this is achieved by switching between geometry and property inversion after each iteration. An example of combined geometry and property inversion, constrained by pierce points and downhole susceptibility logs, is described in this section.

The Bull Creek prospect is located near Cloncurry, Queensland (Figure 5). The Proterozoic basement is overlain unconformably by 30-50m of black shales. The mineralisation and alteration history of Bull Creek has been reviewed by Hart & Lane (2001). Sparse drilling defined magnetite-pyrrhotite mineralisation bearing some similarity to that at the nearby Eloise deposit. Gridded ground magnetic data is depicted in Figure 11; the peak magnetic response exceeds 4000 nT. Susceptibility recorded downhole ranges between 0.1 and 0.8 SI.

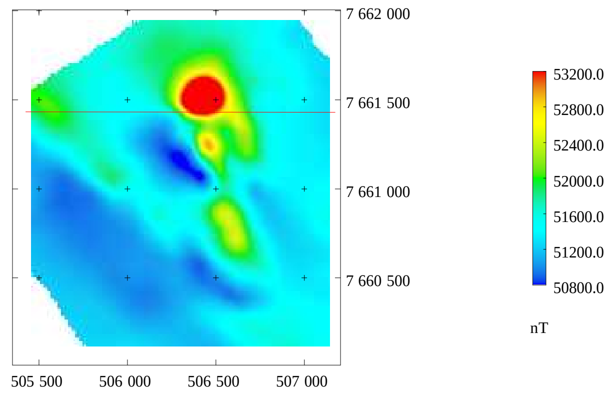


**Figure 11:** Bull Creek total magnetic intensity image, based on ground readings. (Data courtesy Exco Resources).

The starting model for inversion comprised three simple bodies, shaped in Gocad so as to enclose the susceptible intersections in each drill hole. Most drill holes defined a single intersection of higher susceptibilities; consequently a layer of susceptibility spanning the entire model area was modelled from these intersections. One drill hole (BCD-002) encountered three intervals of moderate to high susceptibility and prompted inclusion of two additional bodies of limited lateral extent, above and below the extensive magnetic horizon (Figure 12).

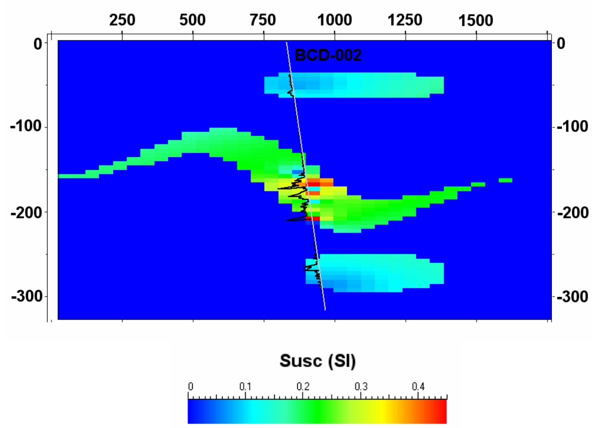


**Figure 12:** EW cross-section (7661425mN; marked in Figure 11) illustrating the three susceptible bodies in the starting model in relation to the BCD-002 drill hole. Downhole susceptibility logs shown in black. Drill hole is oblique and has been projected onto the section. Vertical exaggeration 1:3.

Magnetic susceptibility data were upscaled to the model cell size (50 x 50 x 5m) via simple averaging of all susceptibility measurements within each block model cell. Susceptibility was then distributed within each magnetic unit of the starting model via inverse distance squared weighting of the upscaled susceptibility logs.

Both the shape and susceptibility distribution of the magnetic bodies were altered during inversion. Drill hole pierce points and (upscaled) susceptibilities were fixed. The BCD-002 section after inversion is illustrated in Figure 13. The main magnetic horizon has been transformed from a sigmoid to an arch on this section, with high susceptibility in the west as well as the east. The changes to the deep magnetic body are primarily geometrical: it has merged with the main magnetic horizon, but its susceptibility has remained low. By contrast, the shallow body has developed high susceptibility away from the drill hole, but its shape is little different after inversion.

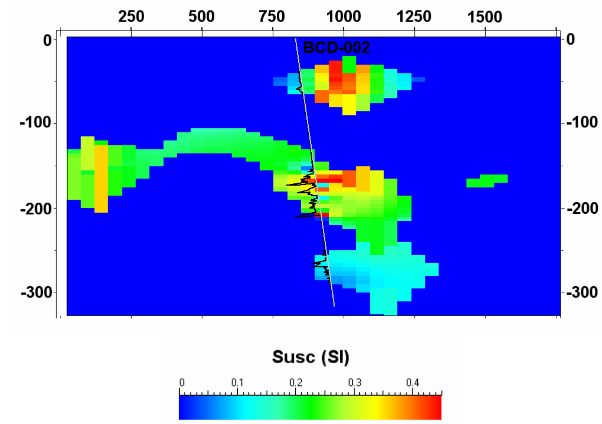


**Figure 13:** EW cross-section (7661425mN, marked in Figure 11) illustrating the susceptibility model after combined geometry and property inversion. Downhole susceptibility logs shown in black. Drill hole BCD-002 is oblique and has been projected onto the section. Vertical exaggeration 1:3.

The lateral variation in susceptibility through the model is illustrated in Figure 14, the cells comprising the magnetic bodies are coloured according to susceptibility.

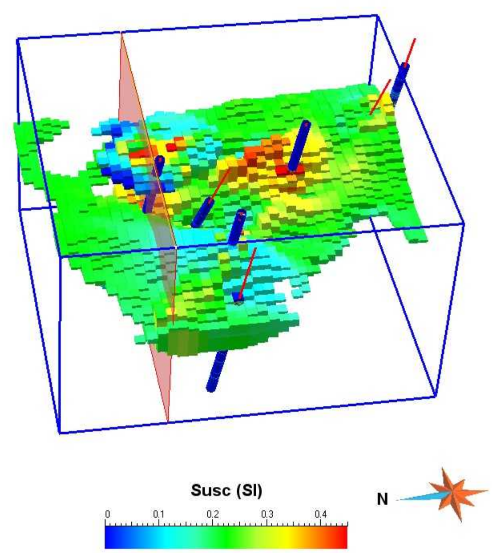


**Figure 14:** Cells within the magnetic bodies, coloured by susceptibility, after combined geometry and property inversion. Drill holes with susceptibility measurements are shown. The location of the cross-section depicted in Figures 12 and 13 is indicated by transparent plane.

The initial RMS data misfit of 418 nT was reduced to 24 nT by constrained geometry and property inversion. The computed response of the inverted model (Figure 15) compares favourably with the observed data (Figure 11).

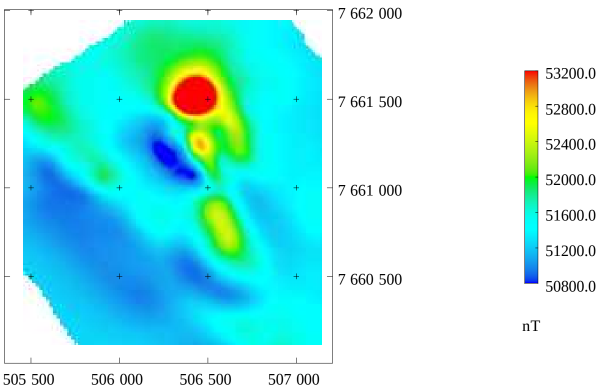


**Figure 15:** Computed TMI response of the Bull Creek model after combined geometry and property inversions.

From a fairly simple, rapidly constructed starting model, the inversion has defined two magnetic bodies, consistent with drill hole pierce points and with downhole susceptibility measurements, which can account for the magnetic data. Inversion has defined some high susceptibility zones not intersected by the existing drill holes, e.g. east of BCD-002 (Figure 13). These might constitute follow-up drill targets.

## Constrained property inversion of TMI, Cannington, Queensland

### Introduction

The Cannington silver-lead-zinc mine is located in the Eastern Succession of the Mount Isa Inlier in northwestern Queensland, Australia (Figure 5). It is a Broken Hill style deposit (Walters & Bailey, 1998), and is one of the largest silver producers in the world. Cannington was discovered by BHP Minerals in 1990 as a result of exploration focussed on discrete magnetic anomalies (Walters, 1998). The mineralisation is hosted in quartzo-feldspathic gneisses. The geological structure at Cannington is complex, involving fault terminations of an isoclinal syncline.

Given the close association between economic sulphides with magnetite and pyrrhotite at Cannington, it is of some importance to fully explain the magnetic signature of the deposit. The technical objective is to improve the understanding of the sub-surface 3D magnetic susceptibility distribution; the exploration objective is to assess whether there are any unexplained magnetic features (possible drill targets). The magnetic response of Cannington has been the subject of two previous studies, namely Huynh (2001) and Fullagar & Pears (2003). In the work described here, core and downhole susceptibility data are used as explicit "hard" constraints on the sub-surface susceptibility; previously, the susceptibility data constrained the inversion only in a general way, as the basis for selection of starting values and bounds.

Ground magnetic data had been collected over Cannington prior to commencement of mining (Figure 16). The data, now gridded to 20m by 20m, are understood to be a composite from a number of surveys. The magnetic signatures of the shallow, lower-grade northern zone and deeper, higher-grade southern zone are clearly distinguishable. The main southern anomaly has a peak amplitude of approximately 2000nT.

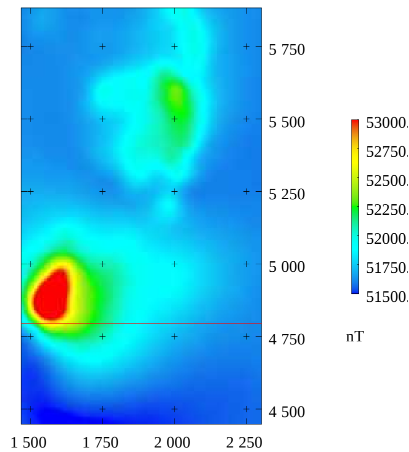


**Figure 16:** Observed TMI (ground magnetics) over Cannington.

Inversion is constrained by the known geological structure, and by individual magnetic susceptibility values. The susceptibility data were used in two ways: to characterise the susceptibility distribution within each geological unit, and to constrain the susceptibility locally within neighbourhoods surrounding the core measurements. A 3D block model was provided by BHP Billiton. In this model, the geology was represented in terms of mineralisation types and host lithologies. The magnetic characteristics of the mineralisation types are summarised in Table 2. The mineralisation types have been sub-divided into northern and southern styles (Table 3). The block size was variable in the original Datamine model; this model was re-cast into regular 10 x 10 x 10m cells using Gocad. Representative vertical and horizontal sections through the deposit are presented in Figure 17.

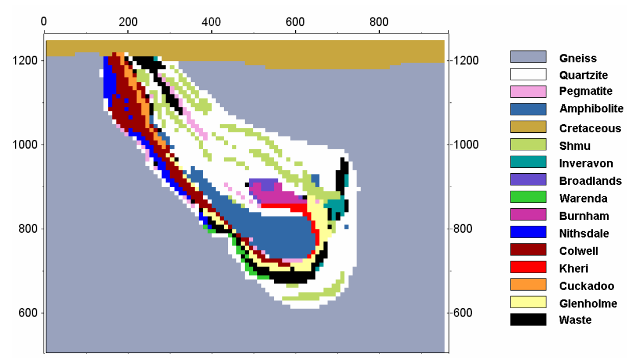


**Figure 17a:** EW cross-section 4795N, illustrating Cannington geology. Red line in Figure 16 marks the section location. Colours refer to mineralisation types. Horizontal axis represents distance from western edge of model.

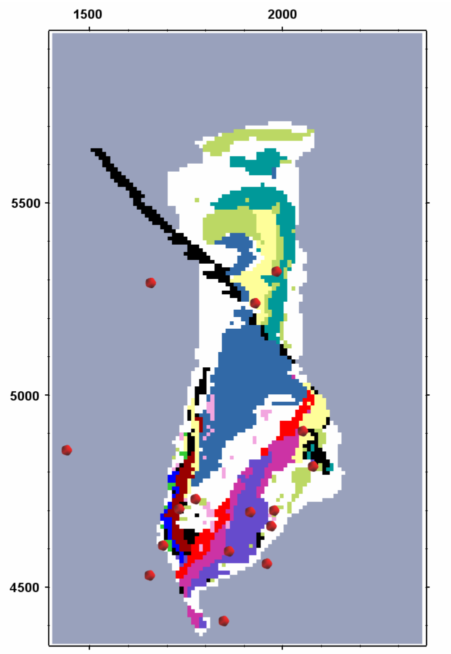


**Figure 17b:** Horizontal section at RL 895m, illustrating Cannington geology. Colours refer to mineralisation types (Figure 17a). Red dots mark intersection points, at this level, for holes from which susceptibility readings were derived. NW-SE striking Treppel Fault zone shown in black.

About 6000 susceptibility measurements have been taken at Cannington, mostly during feasibility drilling. The vast majority of the susceptibility readings refer to 1m drill core samples; the remainder were derived via downhole susceptibility logging. The holes for which susceptibility data exist are distributed reasonably well across both northern and southern zones of the deposits (Figure 17b), but their overall spatial density is relatively sparse, e.g. in comparison to the assays. However, relative to many other mine sites, the susceptibility data base at Cannington is very substantial.

The susceptibility data had been recorded early in the life of the mine, before the mineralisation type classification had matured and before mineralisation logging was performed routinely. In the absence of reliable visual logs, the susceptibility readings could not be directly related to mineralisation types. As a fallback option, the susceptibility readings were assigned to mineralisation types according to the location of the readings within the block model of the orebody. This is far from ideal, but is the only practical approach under the circumstances.

The inadequacies of the indirect geological control are evident from inspection of Figure 18, which shows drill hole susceptibility histograms for Broadlands and Burnham (1m intervals). The distribution for Broadlands (Figure 18a) is reasonably consistent with expectations, except for the high susceptibility tail. However, the distribution for Burnham (Figure 18b) includes far too many low susceptibility values for a mineralisation characterised by abundant magnetite (Table 2).

**Table 2: Cannington mineralisation types**

| **Mineralisation type** | **Ore type** | **Magnetic Mineralogy** | **Magnetic character**<br>Weak: below 10 x 10-3 SI<br>Moderate: 10 – 100x10-3 SI<br>High: above 100 x 10-3 SI |
|---|---|---|---|
| **Broadlands** | Low-medium grade<br>Pb >> Zn | - | Non to weakly magnetic |
| **Burnham** | High grade<br>Pb >> Zn | Abundant magnetite<br>Trace pyrrhotite | Highly magnetic |
| **Colwell** | Medium-high grade<br>Zn > Pb | Abundant magnetite | Highly magnetic |
| **Cukadoo** | Low-medium grade<br>Zn > Pb | - | Non to weakly magnetic |
| **Glenholme** | High grade<br>Pb ~ Zn | - | Non to weakly magnetic |
| **Glenholme Breccia** | Very high grade<br>Pb ~ Zn | Trace pyrrhotite | Non to weakly magnetic |
| **Inveravon** | Low grade<br>Pb > Zn | - | Non to weakly magnetic |
| **Kheri** | Low grade<br>Zn > Pb | Minor magnetite<br>Minor pyrrhotite | Weakly to moderately magnetic |
| **Nithsdale** | Medium grade<br>Pb >> Zn | Abundant magnetite<br>Trace pyrrhotite | Highly magnetic |
| **Warenda** | Low grade<br>Pb > Zn | - | Non to weakly magnetic |

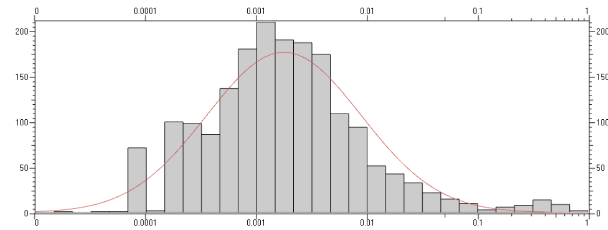

a) Susceptibility (SI)

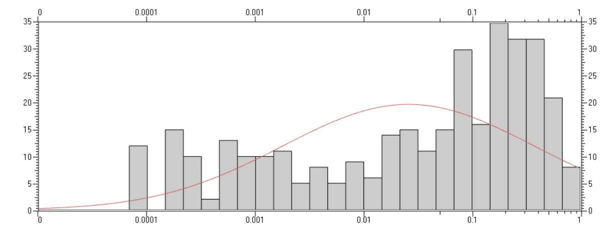

b) Susceptibility (SI)

**Figure 18:** Histograms for drill hole susceptibility data (1m intervals) for (a) Broadlands and (b) Burnham mineralisation, based on 1875 and 345 readings, respectively.

Very high susceptibilities (greater than 1 SI) are notably absent from the compilation. This is attributed to removal of high grade core intervals for assaying, and to an upper limit of 1 SI for the hand-held susceptibility meter. Consequently, the core susceptibility distributions for the most magnetic units are somewhat biased towards lower values (Fullagar, 2002).

A satisfactory fit between observed and calculated total magnetic intensity (TMI) was achieved in two stages of inversion of the ground magnetic data using VPmg. In the first stage of inversion, susceptibilities of individual mineralisation types were assumed uniform; in the second stage the susceptibility was allowed to become heterogeneous within individual units, subject to drill core susceptibility readings. The two inversions are described in turn below. Only the susceptibility was adjusted during inversion in both cases; the model geometry was fixed. Ambient geomagnetic field parameters were as follows: amplitude 51114nT, inclination -51.44$^{o}$, and declination 6.13$^{o}$.

## Homogeneous property inversion

During homogeneous unit inversion, the magnetic susceptibility of each geological unit was adjusted in order to improve the fit between the measured data and the calculated TMI. The inversion problem *per se* was small, involving only 22 parameters (the susceptibilities of the different host lithologies and mineralisation types); Cretaceous cover and gneiss played no part. Consequently the homogeneous property inversion is computationally fast, notwithstanding that there are 3542 data and 1175328 model cells.

The individual susceptibilities before and after homogeneous unit inversion, and the susceptibility bounds, are recorded in Table 3. Susceptibility bounds were assigned on the basis of analysis of all the 1m susceptibility readings, from both core and downhole logs (Fullagar, 2002). The lower bound was defined as the 16th percentile value in each case; the upper bound was defined as the 84th percentile value. The upper bounds for a number of the mineralisation types are rather high, given the descriptions in Table 2; in particular, the maxima for Warenda and Kheri are incompatible with the geological classification. This is a consequence of the crude manner in which the susceptibility data were related to mineralisation types.

**TABLE 3: Initial, Minimum, Maximum, and Inverted Susceptibilities**

| UNIT | Initial Susc. (10-3SI) | Lower Susc. Bound (10-3SI) | Upper Susc. Bound (10-3SI) | Susc. after Homog inversion (10-3SI) |
|---|---|---|---|---|
| Cretaceous cover | 0 | 0 | 0 | 0 |
| | | | | |
| Southern Zone | | | | |
| Gneiss | 0 | 0 | 0 | 0 |
| Quartzite | 0.15 | 0 | 1 | 1 |
| Schmu | 1 | 0 | 1 | 1 |
| Amphibolite | 0 | 0 | 1 | 0 |
| Pegmatite | 2.7 | 0 | 5 | 5 |
| Inveravon | 2 | 1 | 7 | 2.6 |
| Broadlands | 25 | 4 | 265 | 73.9 |
| Warenda | 207 | 11 | 1212 | 217.3 |
| Burnham | 241 | 233 | 852 | 293.7 |
| Nithsdale | 343 | 250 | 1291 | 472.0 |
| Colwell | 218 | 107 | 992 | 388.1 |
| Kheri | 289 | 263 | 1032 | 321.0 |
| Cukadoo | 8 | 1 | 85 | 85 |
| Glenholme | 25 | 1 | 319 | 39.7 |
| | | | | |
| Northern Zone | | | | |
| Quartzite_N | 1 | 0 | 1 | 1 |
| Schmu_N | 1 | 0 | 1 | 1 |
| Amphibolite_N | 0 | 0 | 1 | 0 |
| Pegmatite_N | 5 | 0 | 5 | 5 |
| Inveravon_N | 11 | 1 | 155 | 49.9 |
| Broadlands_N | 6 | 1 | 86 | 30.8 |
| Burnham_N | 133 | 75 | 620 | 128.5 |
| Kheri_N | 184 | 60 | 836 | 186.7 |
| Glenholme_N | 1 | 1 | 6 | 1 |

The calculated TMI before and after inversion are shown in Figure 19. The starting model TMI (Figure 19a) bears a qualitative resemblance to the observed TMI (Figure 16), but amplitudes are very low. Inversion has reduced the RMS misfit from 177nT to 132nT in 18 iterations. After inversion, the resemblance between the calculated and observed TMI has improved, but the fit is far from close. The discrepancies are most pronounced over the main southern anomaly. The inversion stalled because there are insufficient degrees of freedom to achieve an acceptable fit to the data, given the constraints imposed, namely fixed geometry, homogeneity of susceptibility, and susceptibility bounds. This stalling behaviour demonstrates that it is not always easy to fit potential field data when geological and petrophysical constraints, based on drilling, are imposed. Thus constrained inversion of potential field data permits discrimination between hypotheses.

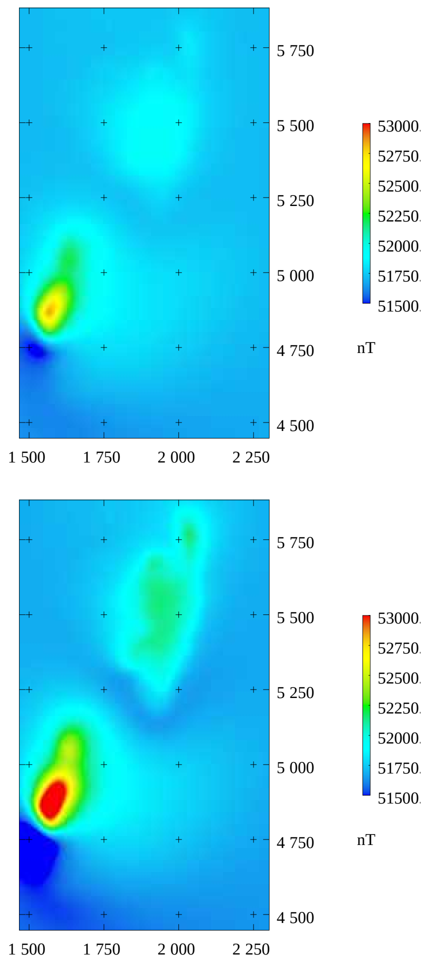


**Figure 19:** Calculated TMI for starting model (top) and after homogeneous unit inversion (bottom)

## Heterogeneous property inversion

The Cannington magnetic data cannot be explained in terms of magnetically homogeneous units. This is not surprising in view of the variability within the mineralised lodes (Walters & Bailey, 1998). Accordingly, a second phase of inversion has been applied, to allow magnetic susceptibility to vary within the mineralised units.

The starting model for heterogeneous property inversion was the homogeneous property model, modified to honour the core susceptibility measurements. The core susceptibility data were interpolated using a Discrete Smooth Interpolation method (Mallet, 1992) to generate a smooth susceptibility grid. Prior to interpolation, the susceptibility data were upscaled; all the 1m susceptibility readings occurring within a given 10m cube were averaged to produce a susceptibility for the cube. This is a crude way to "upscale" 1m linear data to 10m cubic blocks, but more sophisticated approaches would be difficult to justify under the circumstances. The interpolated core susceptibility distribution was then blended with the inverted homogeneous susceptibility model; the influence of each core susceptibility measurements was restricted to a radius of 50m (Figure 20a). More elaborate geostatistical property modelling was not warranted under the circumstances, given the relatively sparse core susceptibility data and the complex geology.

(a)

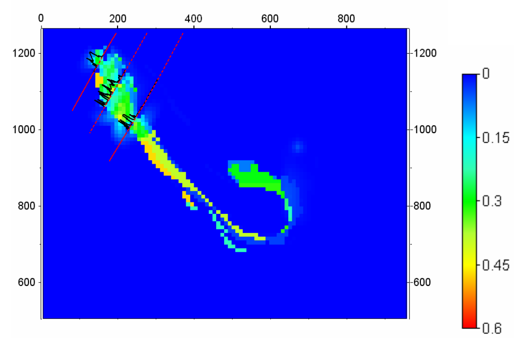


(b)

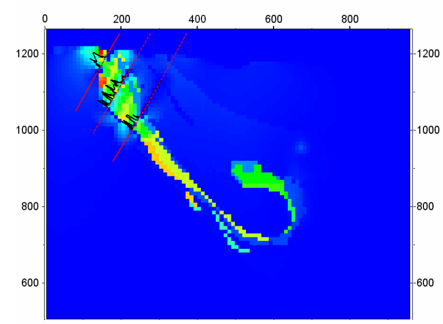


**Figure 20:** Cross-section along 4795N (marked in Figure 16), coloured by susceptibility (SI). Core susceptibility logs (black) and corresponding drill holes (red) superimposed. (a) Starting model for heterogeneous unit inversion, after blending of homogeneous unit susceptibilities with drill hole susceptibilities. (b) Model after heterogeneous unit inversion. Susceptibility has spread into host units, especially into the footwall gneiss at shallow depths.

The interpolation of core susceptibility created zones of elevated susceptibility in host units. During heterogeneous property inversion, the susceptibility of each (10m cube) cell was constrained to lie within a prescribed range, according to its geological unit. Given the "leakage" of susceptibility into host units, the maximum susceptibility for quartzite was increased to 0.5 SI, and the maximum susceptibilities for Schmu (garnet sillimanite schist), amphibolite, and gneiss were increased to 0.15 SI. These high bounds were intended to permit localised "development" of new magnetic bodies in unmineralised host rocks. For all other units, the bounds as defined in Table 3 were unchanged.

Model cells intersected by drill holes for which susceptibility values exist were assigned the average of all core susceptibility readings within that cell. During inversion, the susceptibility of these cells (containing core measurements) was held fixed. VPmg also damped changes in susceptibility for cells within a prescribed "radius of influence" of the fixed cells. The damping decreased linearly with distance from the centre of each fixed cell. Damping factors from different fixed cells combine multiplicatively.

Constrained heterogeneous unit inversion of the Cannington ground magnetics reduced the RMS misfit to 9nT. The calculated TMI after heterogeneous property inversion is shown in Figure 21. The visual resemblance to the measured TMI (Figure 16) is now excellent.

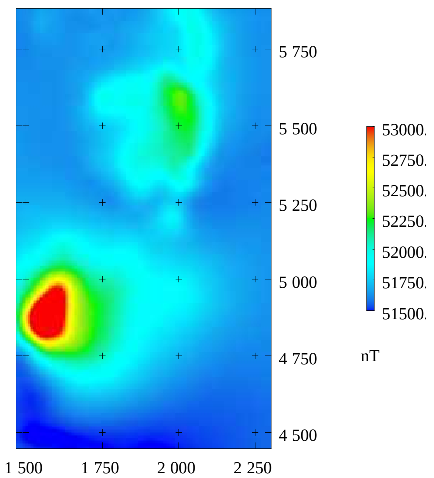


**Figure 21:** Computed TMI after heterogeneous unit inversion. Final RMS misfit is 9nT.

If gneiss is excluded from heterogeneous inversion, and held at a uniform zero susceptibility, a crescent-shaped residual remains, fringing the western margin of the main southern anomaly (Figure 22). In order to account for the residual TMI, inversion has created a new magnetic zone within rock logged as gneiss in the immediate footwall of the main orebody (Figure 20b). This shallow magnetic zone could be real, but it is more probable that the crescent-shaped anomaly is due to self-demagnetisation within the western limb of the syncline.

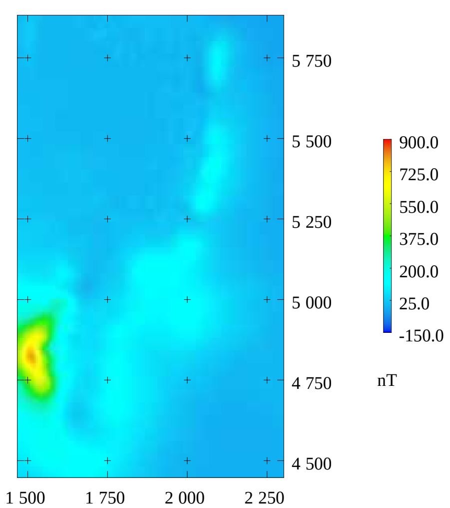


**Figure 22:** Residual TMI after heterogeneous property inversion if susceptibility is fixed at zero in gneiss. The amplitude of the crescent-shaped residual anomaly is ~700 nT.

Susceptibility histograms for Broadlands and Burnham 10m model cells after inversion are presented in Figure 23. The Burnham susceptibility distribution in the inverted model is more consistent with the geological description (Table 2) than the corresponding distribution for drill hole data (Figure 18b).

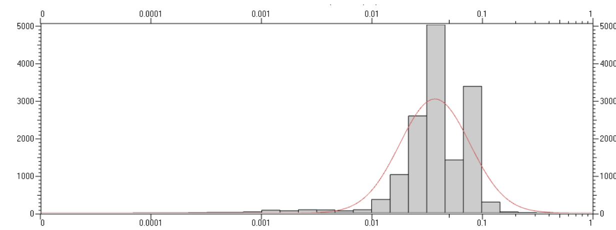


a) Susceptibility (SI)

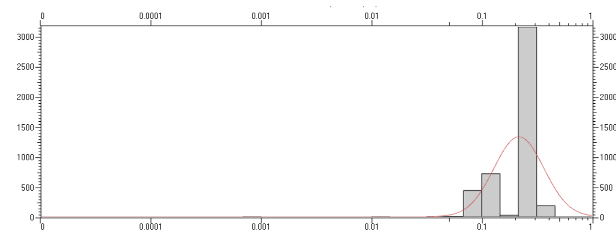


b) Susceptibility (SI)

**Figure 23:** Susceptibility histograms for (a) Broadlands and (b) Burnham mineralisation after inversion based on 14721 and 4582 10m cells respectively. These histograms refer to all model cells classified as either Broadlands or Burnham.

On the other hand, the susceptibility for Broadlands 10m model cells is biased to anomalously high values after heterogeneous unit inversion (Figure 23a), reflecting the high starting value (74 x 10-3 SI) inherited from homogeneous unit inversion. This high value was permitted during homogeneous unit inversion because of the high susceptibility tail in the drill hole susceptibility distribution (Figure 18a). The underlying problem is the imperfect geological control, which has compromised the drill hole susceptibility distributions.

## Conclusions

A susceptibility model has been constructed for the Cannington mine, consistent with the available geological, geophysical, and petrophysical data. The susceptibility model described here is not necessarily the last word on Cannington, both because of the imperfect geological control (with respect to core susceptibility) and because remanence and self-demagnetisation have been ignored. However, the construction of this model illustrates a methodology for constrained inversion at mine sites.

The main lessons from the Cannington inversion are as follows:

1. Constrained inversion of magnetic data over geologically complex mines is feasible, and can highlight unexplained features.
2. Achieving a good fit is not guaranteed during constrained potential fields inversion, rendering it an effective means for creation and testing of hypotheses.
3. Susceptibility data serve two important roles: as point constraints and as members of populations

characterising geological units. At Cannington the impact of the core susceptibility data was blunted, partly because the data were relatively sparsely distributed across the deposit, partly because extremely high susceptibilities were not represented, but mainly as a result of uncertainty about the geological units to which the core samples belonged. Geological control is a crucial ingredient for quantitative interpretation.

## CONCLUSIONS

Interpretation is a shared responsibility of geoscientists, the common goal being an Earth model consistent with all available information. The single unifying model is multi-dimensional, and may include geochemical, geotechnical, and metallurgical attributes in addition to geological and petrophysical attributes. The geophysical inversion model can be regarded as a reduced-dimension "projection" of the complete model, honouring geological and petrophysical observations and fitting the geophysical data. Thus the inversion model should be both a geological model and a petrophysical model.

To date most 3D inversion programs operate on models which are petrophysical but not geological. Geological boundaries and domains cannot be explicitly captured in such models; rather, geology must be inferred from the modified rock property distribution after inversion. In the past decade a small number of 3D potential fields inversion programs has emerged which operate on models which are both geological and petrophysical, i.e. both categorical and quantitative. In addition to incorporating both geology and petrophysics, these programs offer more flexibility and control during inversion. When a starting model is available, they permit geometry inversion as well as property inversion. Inversion can be constrained by drill pierce points and/or property measurements, and can be applied selectively to specific surfaces or rock types. On the other hand, if little or nothing is known about the geology, inversion algorithms based on geological/petrophysical models can perform "unconstrained" property inversion.

In this paper the methodology and application of one 3D potential fields inversion program, VPmg, has been described in some detail. VPmg operates on geological/petrophysical models, i.e. with categorical/continuous parameters. The VPmg model mesh is adaptive to the geology, and deforms as geological surfaces are adjusted during geometry inversion. Both hard and soft constraints are employed to constrain the model geometry and properties. Hard constraints take the form of pierce points, fixed property cells, and upper and lower bounds on surfaces and properties; these ensure that geological core logs and petrophysical measurements are honoured during inversion. Soft constraints take the form of weights, used to suppress rapid changes in the vicinity of pierce points or fixed property cells, or to impose certain characteristics on the spatial property distribution. VPmg default weights are based on simple geometrical considerations, but external weights can be imposed, e.g. based on geostatistical analysis.

The application of VPmg was illustrated in three examples from the Mt. Isa area, Queensland. Regional depth-to-basement interpretation was demonstrated via inversion of gravity data in the first example. Geometry inversion refined an initial estimate of the unconformity surface based on depth-to-source analysis of aeromagnetic data. Best-information densities were assigned to basement lithological domains interpreted from the aeromagnetics. The basement surface was pinned at the two locations where it was known to have been intersected by drill holes. The importance of integrated and constrained interpretation was demonstrated: the interpreted basement topography is almost a mirror image when constraints are removed. Gravity lows are ultimately attributed to shallow granites and felsic rocks in the basement, not to thick cover. Thus constrained inversion can strongly influence area selection for exploration.

In the second example, combined geometry and property inversion is illustrated over an exploration prospect. A starting model comprising three magnetic units was constructed from down hole susceptibility measurements from 6 drill holes. During inversion, the magnetic units were allowed to change in shape and to develop heterogeneity in susceptibility (subject to the property and geometry constraints imposed by drilling) in order to fit the data. This approach permits rapid quantitative interpretation of magnetically susceptible (or dense) bodies in a manner that explicitly honours all drill hole information. An inferred shallow high susceptibility zone constitutes a possible exploration target.

In the third example, constrained property inversion is applied to ground magnetic data recorded over the Cannington Ag-Pb-Zn mine. Initially the susceptibility of each model unit was assumed homogeneous, and the optimal susceptibility values were determined. Subsequently, the susceptibility of each unit was allowed to become heterogeneous. Susceptibility was constrained locally by drill core susceptibility measurements. However, uncertainty about the mineralisation type to which susceptibility measurements belonged distorted the susceptibility distributions, and hence translated into uncertainty in the upper and lower property bounds. Thus, incomplete geological logging compromised the geophysical inversion. Nonetheless, the exercise demonstrated that constrained inversion of magnetic data over geologically complex mines is feasible, and can highlight potential drill targets, e.g. magnetic mineralisation in normally non-magnetic stratigraphy.

In the next decade, some developments can be predicted with confidence. Computers will continue to increase in power, and the advent of 64-bit systems will offer an immense expansion of addressable memory. Inversion speed per se will wane as an issue, both because of hardware improvements and because stochastic and steepest descent inversion algorithms are inherently fast. Forward modelling and calculation of sensitivities will be the rate-limiting factor. Combined inversion of surface, airborne, and downhole data will be commonplace. Greater volumes of petrophysical data will allow more complete spatial characterisation of rock properties, thereby expanding the role of geostatistical techniques for property modelling. However, upscaling will continue to exercise minds. Joint inversions, even those involving 3D electromagnetic or seismic inversion, will be computationally feasible, but the complexity of the underlying cross-property relationships will probably dictate that most multi-property inversions are still performed sequentially rather than simultaneously. Finally, managers will increasingly demand an additional level of sophistication, requiring their geoscientists to not only produce an interpretation consistent with all available data, but also to quantify the uncertainty in the interpretation, so that decision-making is fully informed and risks are minimised. To this end, geologically realistic inversion could be envisaged as a specialised combination of geological and petrophysical modelling, constrained by geophysics, which defines equally probable but possibly disparate geological interpretations.

## ACKNOWLEDGEMENTS

The Cannington and Bull Creek inversion examples are published by kind permission of BHP Billiton Minerals Pty Ltd and Exco Resources N.L. respectively. We are grateful to Mike Barlow (BHP Billiton) for his support and for reviewing the Cannington section. Our thanks also to Bill Morris (McMaster University) for his patience, encouragement, and technical review.

## REFERENCES

Bosch, M., Guillen, A., and Ledru, P., 1999, Lithologic tomography – an application to geophysical data from the Cadomian belt of northern Brittany, France: Tectonophysics, 331, 197-227.

Bosch, M., Meza, R., Jimenez, R., and Honig, A., 2006, Joint gravity and magnetic inversion in 3D using Monte Carlo methods: Geophysics, 71, G153-G156.

Chasseriau, P, and Chouteau, M., 2003, 3D gravity inversion using a model of parameter covariance: J. Appl. Geophys., 52, 59-74.

Close, D.I., Roach, M.J., Bishop, J.R., and Lewis, R.J.G., 2001, Electrical properties of porphyry mineralisation at the Cadia Ridgeway gold-copper deposit, New South Wales – implications for exploration: Exploration Geophysics, 32, 141-146.

Dubrule, O., 2003, Geostatistics for seismic data integration in Earth models: SEG/EAGE Distinguished Instructor Series No. 6.

Fullagar, P.K., 2000, The expanding role of mine geophysics: Proc. 4th Intl. Mining Geology Conference, AusIMM Publication 3/2000, 301-314.

Fullagar, P.K., 2002, Magnetic susceptibility of mineralisation types at Cannington, Queensland: Fullagar Geophysics Pty Ltd Report BH01F-4.

Fullagar, P.K., and Pears, G.A., 2003, Drilling-constrained 3D inversion of Cannington ground magnetics and provisional blind targeting: Fullagar Geophysics/ Mira Geoscience Report BH01F-6.

Fullagar, P.K., Hughes, N.A., and Paine, J., 2000, Drilling constrained 3D gravity inversion: Exploration Geophysics, 31, 17-23.

Fullagar, P.K., Pears, G.A., Hutton, D., and Thompson, A., 2004, 3D Gravity and Aeromagnetic Inversion for MVT Lead-Zinc Exploration at Pillara, Western Australia: Exploration Geophysics, 35, 142-146.

Fullagar, P.K., Pears, G.A., and McMonnies, B., 2006, Constrained inversion of geological surfaces - pushing the boundaries: in R.J.L. Lane, editor, Geologically realistic inversion of gravity and magnetic data from the Australian Earth Sciences Convention 2006 Workshop: Geoscience Australia Record (in preparation).

Hart, J., and Lane, R., 2001, Comparison of Airborne and Ground TEM systems for a conductor beneath conductive cover - an example from North-West Queensland, Australia: Extended Abstract, 15th ASEG International Geophysical Conference and Exhibition, Brisbane, August, 2001.

Hone, I.G., Carberry, V.P. and Reith, H.G., 1987, Physical property measurements on rock samples from the Mt Isa Inlier, northwest Queensland: BMR Report 265, Canberra.

Huynh, T.H., 2001, Three-dimensional geological and geophysical modelling of the Cannington Deposit, NW Queensland, Australia: M.Sc. thesis, Australian Crustal Research Centre, Monash University.

Lane, R., Seikel, R., and Guillen, A., 2006, Exploration of alternate 3D geological maps guided by gravity and magnetic data: in R.J.L. Lane, editor, Geologically realistic inversion of gravity and magnetic data from the Australian Earth Sciences Convention 2006 Workshop: Geoscience Australia Record (in preparation).

Li, Y., and Oldenburg, D.W., 1996, 3D inversion of magnetic data: Geophysics, 61, 394-408.

Li, Y., and Oldenburg, D.W., 1998, 3-D inversion of gravity data: Geophysics, 63, 109-119.

Mackey, T.E., Gunn, P.J., Meixner, A.J. and Blake, D.H., 1999, Boulia, interpreted geology, (1:250 000 scale map), AGSO.

Mackey, T.E., Gunn, P.J., Meixner, A.J. and Blake, D.H., 2000, Mapping Australian geolgoy under cover: a case study applied to the Boulia and Springvale 1:250000 map sheets, Queensland: ASEG Preview No. 87, August 2000, pp28-32.

Mallet, J.L., 1992. Discrete smooth interpolation in geometric modelling: Computer Aided Design, 24, 178-191.

McGaughey, J., 2006, The Common Earth Model: A Revolution in Mineral Exploration Data Integration: in GIS Applications in the Earth Sciences, Geological Association of Canada Special Publication #44, edited by J.R. Harris, 567-576.

Oz, B., Deutsch, C.V., and Frykman, P., 2002, A visual basic program for histogram and variogram scaling: Computers & Geosciences, 28, 21–31.

Pears, G.A., Fullagar, P.K., and Andrews, P., 2001, 3D gravity modelling and interpretation for the 1:250,000 Boulia map sheet, Queensland: Extended Abstract, 15th ASEG International Geophysical Conference and Exhibition, Brisbane, August, 2001.

Walters, S.G., 1998, Broken Hill type deposits: AGSO Journal of Australian Geology & Geophysics, 17, 229-237.

Walters, S., and Bailey, A., 1998, Geology and mineralisation of the Cannington Ag-Pb-Zn deposit – an example of Broken Hill type mineralisation in the Eastern Succession, Mount Isa Inlier, Australia: Economic Geology, 93, 1307-1329.